$V = 1475\,(3)$ Å^3
$Z = 4$
$D_x = 6.66$ Mg m^{-3}
$D_m = 6.66$ Mg m^{-3}

$T = 370$ K
Sphere
0.3 mm (radius)
Colourless

Data collection

Enraf–Nonius CAD-4 diffractometer
ω/θ scans
Absorption correction: by spherical model
$T_{\min} = 0.0009$, $T_{\max} = 0.0185$
5787 measured reflections
1715 independent reflections
1314 observed reflections $[I > 3\sigma(I)]$

$R_{\text{int}} = 0.065$
$\theta_{\max} = 30°$
$h = -20 \rightarrow 20$
$k = -20 \rightarrow 20$
$l = 0 \rightarrow 10$
3 standard reflections monitored every 200 reflections intensity decay: <4%

Refinement

Refinement on F
$R = 0.053$
$wR = 0.058$
$S = 1.12$
1115 reflections
52 parameters
$w = (weight)[1-(\Delta F/6\sigma^2(F)]^2$

$(\Delta/\sigma)_{\max} = 0.01$
$\Delta\rho_{\max} = 5$ e Å^{-3}
$\Delta\rho_{\min} = -6$ e Å^{-3}
Extinction correction: none
Atomic scattering factors from Cromer & Waber (1974)

Table 1. *Fractional atomic coordinates and equivalent isotropic displacement parameters* (Å^2)

$$U_{\text{eq}} = (1/3)\Sigma_i\Sigma_j U_{ij}a_i^*a_j^*\mathbf{a}_i.\mathbf{a}_j.$$

	x	y	z	U_{eq}
Pb1	0.08474 (7)	−0.23970 (6)	0	0.018 (1)
Pb2	−0.06116 (6)	−0.21768 (5)	1/2	0.013 (2)
Pb3	0	1/2	1/4	0.072 (2)
Al1	0.1581 (4)	0.3255 (4)	0	0.012 (4)
Al2	0	0	0.2460 (1)	0.012 (4)
F1	0	0	0	0.038 (5)
F2	0	0	1/2	0.038 (5)
F3	0.3854 (9)	0.4500 (8)	0.2460 (2)	0.038 (5)
F4	0.2001 (9)	0.4076 (9)	0.1730 (2)	0.038 (5)
F5	0.3921 (9)	0.2494 (9)	0.6700 (2)	0.038 (5)
F6	0.2630 (10)	0.2610 (10)	0	0.038 (5)
F7	0.4530 (10)	0.1120 (10)	1/2	0.038 (5)
F8	0.4170 (10)	0.1250 (10)	0	0.038 (5)

Table 2. *Selected geometric parameters* (Å, °)

Pb1···F4^{i}	2.52 (1)	Al1—F4^{xi}	1.82 (1)
Pb1···F4^{ii}	2.52 (1)	Al1—F5^{vii}	1.78 (1)
Pb1···F6^{iii}	2.54 (2)	Al1—F5^{xii}	1.78 (1)
Pb2···F5^{iv}	2.52 (1)	Al1—F6	1.75 (2)
Pb2···F5^{v}	2.52 (1)	Al1—F7^{vii}	1.81 (2)
Pb2···F6^{vi}	2.54 (2)	Al2—F1	1.777 (8)
Pb2···F8^{vi}	2.27 (2)	Al2—F2	1.836 (8)
Pb3···F7^{vii}	2.51 (1)	Al2—F3^{vii}	1.79 (1)
Pb3···F7^{viii}	2.51 (1)	Al2—F3^{xiii}	1.79 (1)
Pb3···F7^{ix}	2.51 (1)	Al2—F3^{xiv}	1.79 (1)
Pb3···F7^{x}	2.51 (1)	Al2—F3^{i}	1.79 (1)
Al1—F4	1.82 (1)		
F4^{i}···Pb1···F4^{ii}	139.7 (6)	F4—Al1—F5^{xii}	92.7 (6)
F4^{ii}···Pb1···F6^{iii}	85.0 (3)	F5^{xii}—Al1—F5^{vii}	87.2 (9)
F5^{v}···Pb2···F5^{iv}	142.2 (6)	F4—Al1—F6	93.3 (6)
F5^{v}···Pb2···F6^{vi}	73.4 (3)	F4—Al1—F7^{vii}	88.4 (6)
F5^{v}···Pb2···F8^{vi}	77.2 (6)	F5^{vii}—Al1—F7^{vii}	86.8 (6)
F6^{vi}···Pb2···F8^{vi}	75.2 (6)	F6—Al1—F7^{xii}	177.7 (9)
F7^{vii}···Pb3···F7^{viii}	87.9 (6)	F1—Al2—F2	179.99
F7^{ix}···Pb3···F7^{viii}	121.2 (3)	F1—Al2—F3^{vii}	92.0 (5)
F4—Al1^{xi}—F4^{xi}	87.0 (8)	F3^{i}—Al2—F3^{vii}	89.93 (3)
F4—Al1—F5^{vii}	175.1 (7)	F3^{xiii}—Al2—F3^{vii}	176.1 (10)

Symmetry codes: (i) $\frac{1}{2}-y, x-\frac{1}{2}, \frac{1}{2}-z$; (ii) $\frac{1}{2}-y, x-\frac{1}{2}, z-\frac{1}{2}$; (iii) $y, -x, -z$; (iv) $x-\frac{1}{2}, y-\frac{1}{2}, \frac{3}{2}-z$; (v) $x-\frac{1}{2}, y-\frac{1}{2}, z-\frac{1}{2}$; (vi) $x-\frac{1}{2}, y-\frac{1}{2}, \frac{1}{2}+z$; (vii) $\frac{1}{2}-x, \frac{1}{2}-y, \frac{1}{2}-z$; (viii) $x-\frac{1}{2}, \frac{1}{2}+y, \frac{1}{2}-z$; (ix) $-y, x, z$; (x) $y, 1-x, 1-z$; (xi) $x, y, -z$; (xii) $\frac{1}{2}-x, \frac{1}{2}-y, z-\frac{1}{2}$; (xiii) $x-\frac{1}{2}, y-\frac{1}{2}, \frac{1}{2}-z$; (xiv) $y-\frac{1}{2}, \frac{1}{2}-x, \frac{1}{2}-z$.

Data collection: *CAD-4 Software* (Enraf–Nonius, 1989). Cell refinement: *CAD-4 Software*. Data reduction: local program (unpublished). Program(s) used to refine structure: *CRYSTALS* (Watkin, Carruthers & Betteridge, 1985).

The authors wish to thank R. Von der Mühll for piezoelectric and pyroelectric tests and D. J. Watkin for providing the refinement program.

Lists of structure factors, anisotropic displacement parameters and complete geometry have been deposited with the IUCr (Reference: DU1109). Copies may be obtained through The Managing Editor, International Union of Crystallography, 5 Abbey Square, Chester CH1 2HU, England.

References

Andriamampianina, V., Gravereau, P., Ravez, J. & Abrahams, S. C. (1994). *Acta Cryst.* **B50**, 135–141.
Cromer, D. T. & Waber, J. T. (1974). *International Tables for X-ray Crystallography*, Vol. IV, Table 2.2A. Birmingham: Kynoch Press. (Present distributor Kluwer Academic Publishers, Dordrecht.)
Enraf–Nonius (1989). *CAD-4 Software*. Version 5.0. Enraf–Nonius, Delft, The Netherlands.
Ravez, J., Andriamampianina, V. & Abrahams, S. C. (1994). *Ferroelectrics*, **158**, 133–137.
Ravez, J., Andriamampianina, V., Simon, A., Rabardel, L., Ihringer, J. & Abrahams, S. C. (1994). *J. Appl. Cryst.* **27**, 362–368.
Watkin, D. J., Carruthers, J. R. & Betteridge, P. W. (1985). *CRYSTALS User Guide*. Chemical Crystallography Laboratory, Univ. of Oxford, England.

Acta Cryst. (1995). C51, 1732–1735

Octachlorosilasesquioxane, $Cl_8Si_8O_{12}$

KARL WILHELM TÖRNROOS

Structural Chemistry, Stockholm University,
106 91 Stockholm, Sweden

GION CALZAFERRI AND ROMAN IMHOF

Institute for Inorganic and Physical Chemistry,
University of Bern, Freiestrasse 3, CH-3000 Bern 9,
Switzerland

(*Received* 18 *December* 1994; *accepted* 27 *March* 1995)

Abstract

The structure of $Cl_8Si_8O_{12}$ is compared with those of the isostructural compounds $H_8Si_8O_{12}$ and $(CH_3)_8Si_8O_{12}$. The geometric deformations in $Cl_8Si_8O_{12}$ seem to

originate from the joint effect of intermolecular packing interactions (interelectronic repulsion) and electronic factors (electronegativity of the chlorine substituent).

Comment

Octachlorosilasesquioxane, $Cl_8Si_8O_{12}$ (Cl_8T_8), shown in Fig. 1, is essentially isostructural with the previously determined structures of $H_8Si_8O_{12}$ (H_8T_8) at 100 K (Auf der Heyde, Bürgi, Bürgy & Törnroos, 1991) and $(CH_3)_8Si_8O_{12}$ [$(CH_3)_8T_8$] (Koellner & Müller, 1989), but does not retain the non-crystallographic molecular symmetry, T_h ($m\bar{3}$), characteristic of the latter two. The highest attainable molecular symmetry common to the three compounds is O_h ($m\bar{3}m$). As can be seen in Table 2, some of the chemically equivalent, but crystallographically inequivalent structural parameters, notably the tetrahedral angles, differ significantly. Hence, the molecular symmetry is the same as the crystallographic, $S_6(\bar{3})$.

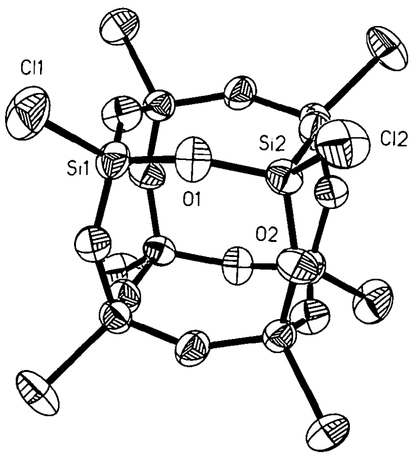

Fig. 1. Structure of the title compound displaying 50% probability anisotropic harmonic displacement ellipsoids and atomic labelling.

The geometric differences between Cl_8T_8, H_8T_8 and $(CH_3)_8T_8$ are as follows (numbers in parentheses represent standard deviation of population, s*). The average Si—O bond distance is shorter, 1.601 (7) Å, compared with 1.618 (1) Å in H_8T_8 and 1.614 (3) Å in $(CH_3)_8T_8$. The angles around the Si atoms in H_8T_8 correspond to those of a regular tetrahedron, which is also true for Cl_8T_8 [109.5 (4)°] when averaging the Si1 and Si2 geometries. However, in contrast to H_8T_8, the individual Si1 and Si2 tetrahedral geometries in Cl_8T_8 are inconsistent, exhibiting a mean exocyclic O—Si1—Cl angle of 109.8 (2)° and a mean endocyclic O—Si1—O angle of 109.1 (2)°, with a mean exocyclic O—Si2—Cl angle of 109.4 (6)° and a mean endocyclic O—Si2—O angle of 109.6 (4)°. The structure of $(CH_3)_8T_8$ has a consistent overall mean exocyclic O—Si—C angle of 109.9 (4)° and a mean endocyclic angle of 109.0 (1)°. The increase in the exocyclic angles is in accord with an interelectronic repulsion scenario, involving orbitals on Cl, CH_3 and the O atoms.

The values given in Table 3 make some further comparisons of the three structures possible. Apart from being, on average, the smallest of the three structures, the non-bonding Si1$\cdots$Si1^{iii} body diagonal distance along the threefold axis in Cl_8T_8 is elongated in relation to the opposite body diagonal distance Si2$\cdots$Si2^{iii}, compared to H_8T_8 and in particular to $(CH_3)_8T_8$. This reveals a deformation of the Si cube towards a more rhombic cage, with a stretching along the threefold axis and a compression perpendicular to it. The deformation is also reflected by the deviating non-bonding Si$\cdots$Si cube-edge distances in Cl_8T_8. The inconsistency between the tetrahedral environment of the two unique Si atoms agrees with this cage deformation.

Apart from the body diagonal distances, the two distances between opposite O atoms across the faces of the cube, O1$\cdots$O5 distances, serve as a sensitive measure of the deviation from O_h symmetry. These differ by as much as 0.308 (1) Å in H_8T_8, while the difference is smaller and essentially identical in Cl_8T_8 [0.078 (7) Å] and $(CH_3)_8T_8$ [0.075 (2) Å].

The deformation of H_8T_8 is attributed to effects of intermolecular Si$\cdots$O interactions, indicative of an incipient nucleophilic attack of O on Si, or of incipient five-coordination of the Si atoms, which have been concluded previously to be largely responsible for deformation effects on silasesquioxane cages (Auf der Heyde, Bürgi, Bürgy & Törnroos, 1991; Bürgi, Törnroos, Calzaferri & Bürgy, 1993; Calzaferri, Imhof & Törnroos, 1994; Törnroos, Bürgi, Calzaferri & Bürgy, 1995). For obvious reasons, such interactions are impossible in the structures of Cl_8T_8 and $(CH_3)_8T_8$, although short intermolecular interactions (less than the sum of the van der Waals radii) are detected in Cl_8T_8 [Cl2$\cdots$Si2($y - \frac{1}{3}, -x + y + \frac{1}{3}, -z + \frac{1}{3}$) and Si2$\cdots$Cl2($x - y + \frac{2}{3}, x + \frac{1}{3}, -z + \frac{1}{3}$) 3.823 (3) Å] and may be the cause of the observed stretching/compression deformation.

Regarding the observed Si—O bond shortening in Cl_8T_8, it seems reasonable to argue that the formal charge of Si must be closer to +4 than in H_8T_8 and $(CH_3)_8T_8$, due to the significant electronegativity of the Cl substituent. The consequently contracted electronic shell of Si results in a shorter Si—O distance, assuming a constant radius of the O atom. This conclusion is indeed qualitatively supported by calculations of the partial charge on Si, using the *Principle of Electronegativity Equalization* by Sanderson (1971), as the partial positive charge on Si increases when going from Si—H *via* Si—CH_3 to Si—Cl.

To circumvent the experimental difficulties resulting from the moisture and X-ray sensitivity of these compounds (Cl_8T_8 in particular), experiments aimed at achieving higher accuracy have to be made at a very

---

* $s = [1/(n-1)][\sum_{i=1}^{n}(x_i - \bar{x})^2]^{1/2}$.

low temperature. Such a low-temperature study of this compound is under preparation, aiming to determine the charge-density distribution, as has been achieved for H_8T_8 at 9.2 K (Törnroos, Schwarzenbach, Larsen & Delley, 1995). Furthermore, additional structure determinations, in particular of $F_8Si_8O_{12}$ and $(OH)_8Si_8O_{12}$, are essential in order to enable a deeper systematic investigation and characterization of the electronic effects on the molecular geometry, in combination with computational methods.

Experimental

The compound was synthesized according to Day, Klemperer, Mainz & Millar (1985) by photochemical chlorination of $H_8Si_8O_{12}$. Small colourless air-sensitive rhombic crystals were grown by slow evaporation from *n*-hexane under an inert atmosphere.

Crystal data

$Cl_8Si_8O_{12}$
$M_r = 700.32$
Trigonal
$R\bar{3}$
$a = 12.353\ (2)$ Å
$c = 12.931\ (2)$ Å
$V = 1708.9\ (4)$ Å^3
$Z = 3$
$D_x = 2.041$ Mg m^{-3}

Mo $K\alpha$ radiation
$\lambda = 0.71073$ Å
Cell parameters from 36 reflections
$\theta = 4.95–11.60°$
$\mu = 1.456$ mm^{-1}
$T = 291\ (2)$ K
Rhombic
0.125 × 0.075 × 0.075 mm
Colourless

Data collection

Stoe AED-2 diffractometer
$\omega/2\theta$ scans
Absorption correction: analytical
$T_{min} = 0.852$, $T_{max} = 0.901$
1117 measured reflections
1117 independent reflections
301 observed reflections $[I > 3\sigma(I)]$

$\theta_{max} = 30.00°$
$h = -8 \rightarrow 17$
$k = -9 \rightarrow 17$
$l = 0 \rightarrow 18$
3 standard reflections
frequency: 180 min
intensity decay: <2.9% (corrected by linear interpolation)

Refinement

Refinement on F^2
$R[F^2 > 2\sigma(F^2)] = 0.0459$
$wR(F^2) = 0.0700$
$S = 1.184$
301 reflections
43 parameters
$w = 1/[\sigma^2(F_o^2) + (0.0261P)^2]$ where $P = (F_o^2 + 2F_c^2)/3$
$(\Delta/\sigma)_{max} < 0.001$

$\Delta\rho_{max} = 0.24$ e Å^{-3}
$\Delta\rho_{min} = -0.40$ e Å^{-3}
Extinction correction: none
Atomic scattering factors from *International Tables for Crystallography* (1992, Vol. C, Tables 4.2.6.8 and 6.1.1.4)

Table 1. *Fractional atomic coordinates and equivalent isotropic displacement parameters* (Å^2)

$$U_{eq} = (1/3)\Sigma_i\Sigma_j U_{ij} a_i^* a_j^* \mathbf{a}_i.\mathbf{a}_j.$$

	x	y	z	U_{eq}
Si1	0	0	0.2072 (3)	0.042 (1)
Si2	0.0129 (2)	0.2096 (2)	0.0686 (2)	0.0396 (6)
Cl1	0	0	0.3611 (3)	0.0742 (15)
Cl2	0.0249 (2)	0.3674 (2)	0.1195 (2)	0.067 (1)
O1	0.0096 (5)	0.1260 (5)	0.1654 (4)	0.049 (2)
O2	0.1317 (5)	0.2441 (5)	−0.0020 (4)	0.0453 (15)

Table 2. *Bond lengths* (Å) *and angles* (°)

Si1—O1^{i}	1.595 (4)	Si2—O2^{iii}	1.605 (4)
Si1—O1	1.595 (4)	Si2—O1	1.610 (4)
Si1—O1^{ii}	1.595 (4)	Si2—Cl2	1.992 (2)
Si1—Cl1	1.989 (4)	O2—Si2^{iv}	1.605 (4)
Si2—O2	1.595 (4)		
O1^{i}—Si1—O1	109.1 (2)	O2—Si2—O1	110.0 (2)
O1^{i}—Si1—O1^{ii}	109.1 (2)	O2^{iii}—Si2—O1	109.0 (2)
O1—Si1—O1^{ii}	109.1 (2)	O2—Si2—Cl2	108.6 (2)
O1^{i}—Si1—Cl1	109.9 (2)	O2^{iii}—Si2—Cl2	109.9 (2)
O1—Si1—Cl1	109.9 (2)	O1—Si2—Cl2	109.7 (2)
O1^{ii}—Si1—Cl1	109.9 (2)	Si1—O1—Si2	148.8 (3)
O2—Si2—O2^{iii}	109.7 (2)	Si2—O2—Si2^{iv}	148.0 (3)

Symmetry codes: (i) $-y, x-y, z$; (ii) $-x+y, -x, z$; (iii) $x-y, x, -z$; (iv) $y, -x+y, -z$.

Table 3. *Non-bonding distances* (Å) *in some octanuclear silasesquioxanes*

	$Cl_8Si_8O_{12}$	$H_8Si_8O_{12}$	$(CH_3)_8Si_8O_{12}$
Si1···Si1^{iii} (Body diagonal of Si_8 cube)	5.359 (8)	5.390 (1)	5.392 (2)
Si2···Si2^{iii} (Body diagonal of Si_8 cube)	5.331 (5)	5.381 (1)	5.392 (1)
O1···O2^{ii} (Across face of Si_8 cube)	3.657 (7)	3.575 (1)	3.679 (2)
O2···O1^{iv} (Across face of Si_8 cube)	3.735 (7)	3.883 (1)	3.754 (2)
Si1···Si2 (Si_8 cube edge)	3.086 (2)	3.109 (1)	3.113 (1)
Si2···Si2^{i} (Si_8 cube edge)	3.077 (2)	3.108 (1)	3.113 (1)

Symmetry codes: (i) $x-y, x, -z$; (ii) $y, -x+y, -z$; (iii) $-x, -y, -z$; (iv) $y-x, -x, z$.

The structure was refined by full-matrix least-squares techniques. Anisotropic displacement parameters were refined for all atoms.

Data collection: *DIF*4 (Stoe & Cie, 1988*a*). Cell refinement: *DIF*4. Data reduction: *REDU*4 (Stoe & Cie, 1988*b*). Program(s) used to solve structure: *SHELXS*86 (Sheldrick, 1990). Program(s) used to refine structure: *SHELXL*93 (Sheldrick, 1993). Molecular graphics: *SHELXTL-Plus* (Sheldrick, 1991).

This project is financially supported by the Swedish Natural Science Research Council and by the Schweizerischer Nationalfonds zur Förderung der wissenschaftlichen Forschung.

Lists of structure factors, anisotropic displacement parameters and complete geometry have been deposited with the IUCr (Reference: AB1255). Copies may be obtained through The Managing Editor, International Union of Crystallography, 5 Abbey Square, Chester CH1 2HU, England.

References

Auf der Heyde, T. P. E., Bürgi, H.-B., Bürgy, H. & Törnroos, K. W. (1991). *Chimia*, **45**, 38–40.
Bürgi, H.-B., Törnroos, K. W., Calzaferri, G. & Bürgy, H. (1993). *Inorg. Chem.* **32**, 4914–4919.
Calzaferri, G., Imhof, R. & Törnroos, K. W. (1994). *J. Chem. Soc. Dalton Trans.* pp. 3123–3128.
Day, V. W., Klemperer, W. G., Mainz, V. V. & Millar, D. M. (1985). *J. Am. Chem. Soc.* **107**, 8262–8264.

Koellner, G. & Müller, U. (1989). *Acta Cryst.* C**45**, 1106–1107.
Sanderson, R. T. (1971). *Chemical Bonds and Bond Energies*, pp. 13–25. New York: Academic Press.
Sheldrick, G. M. (1990). *Acta Cryst.* A**46**, 467–473.
Sheldrick, G. M. (1991). *SHELXTL-Plus*. Release 4.1. Siemens Analytical X-ray Instruments Inc., Madison, Wisconsin, USA.
Sheldrick, G. M. (1993). *SHELXL93. Program for the Refinement of Crystal Structures*. Univ. of Göttingen, Germany.
Stoe & Cie (1988*a*). *DIF4. Diffractometer Control Program*. Version 6.2. Stoe & Cie, Darmstadt, Germany.
Stoe & Cie (1988*b*). *REDU4. Data Reduction Program*. Version 6.2. Stoe & Cie, Darmstadt, Germany.
Törnroos, K. W., Bürgi, H.-B., Calzaferri, G. & Bürgy, H. (1995). *Acta Cryst.* B**51**, 155–161.
Törnroos, K. W., Schwarzenbach, D., Larsen, F. K. & Delley, B. (1995). *Acta Cryst.* B**51**. In preparation.

Acta Cryst. (1995). C**51**, 1735–1737

$Li_{1.14}Nb_{0.93}Sc_{0.67}Cr_{0.40}(PO_4)_3$

SYLVIE RIVIER, JACQUES ANGENAULT AND
JEAN-CLAUDE COUTURIER

Laboratoire de Cristallochimie du Solide, CNRS-URA 1388, Université Pierre et Marie Curie, 4 Place Jussieu, Paris CEDEX 05, France

FRANCIS ROBERT

Laboratoire de Chimie des Métaux de Transition, CNRS-URA 419, Université Pierre et Marie Curie, 4 Place Jussieu, Paris CEDEX 05, France

MICHEL QUARTON

Laboratoire de Cristallochimie du Solide, CNRS-URA 1388, Université Pierre et Marie Curie, 4 Place Jussieu, Paris CEDEX 05, France

Abstract

Lithium niobium scandium–chromium tris(monophosphate) presents a large domain of homogeneity by cationic substitution: $Nb^V = Sc^{III}(Cr^{III}) + 2Li^I$. Basic structural units comprise two MO_6 octahedra linked by three PO_4 tetrahedra, as in the Nasicon-type structure, with partial ordering of the M atoms (M = Nb, Sc, Cr). Li^+ cations partially occupy interstices of two kinds, connected by channels along the c axis with small windows which limit the ionic mobility.

Comment

Compounds forming Nasicon (the acronym for Na superionic conductor) or related structures constitute a very large class of solid-state compounds because Zr in $NaZr_2(PO_4)_3$ can be substituted by many cations. In the course of studies concerning Nasicon-type Li ionic conductors, three extremes of cationic conductivity values at 573 K were found for $Li_{1+x}Ti_{2-x}In_x(PO_4)_3$, correlated with the existence of three distinct phases: phase I for $0 \leq x \leq 0.4$ (space group $R\bar{3}c$), phase II for $0.4 < x < 1.1$ ($Pbca$) and phase III for $1.1 \leq x \leq 2$ ($P2_1/n$) (Hamdoune, Tran Qui & Schouler, 1986). Phases I and II are found in $Li_{1-x}Ti^{IV}_{2-x}Ti^{III}_x(PO_4)_3$ for $0 \leq x \leq 0.5$ and $0.5 < x < 1.2$, respectively (Wang, Greenblatt, Wang & Hwu, 1993). The covalency of Ti^{IV}—O bonds weakens Li—O interactions and so favours ionic conductivity.

In order to increase covalency of the structural skeleton $[M_2(PO_4)_3]$, we have introduced a cation in a pentavalent oxidation state: $Li_{2(x+y)-1}Nb^V_{2-x-y}Sc^{III}_xCr^{III}_y(PO_4)_3$ presents a large domain of homogeneity for $x + y > 0.5$. We describe the crystal structure of this phase for $x = 0.674$ and $y = 0.394$.

The $[M_2(PO_4)_3]$ framework consists of irregular MO_6 octahedra and PO_4 tetrahedra (Table 2). Like the Nasicon structure (Hagman & Kierkegaard, 1968), the basic unit includes two MO_6 octahedra linked by three PO_4 tetrahedra (Fig. 1). These units are distorted and they reveal partial cationic ordering: Nb and Cr atoms located in $M(1)O_6$ octahedra, Nb and Sc atoms in $M(2)O_6$ octahedra. The M—O distances in the $M(1)O_6$ octahedra are significantly shorter than the M—O distances in the $M(2)O_6$ octahedra, in accord with the values of the ionic radii: $r_{Nb^{5+}} = 0.64$, $r_{Cr^{3+}} = 0.615$ and $r_{Sc^{3+}} = 0.745$ Å (Shannon, 1976). Two parallel units $[M(1)M(2)P_3O_{18}]$ share two corner O atoms, thus constituting double units $[M(1)_2M(2)_2P_6O_{34}]$ (Fig. 1).

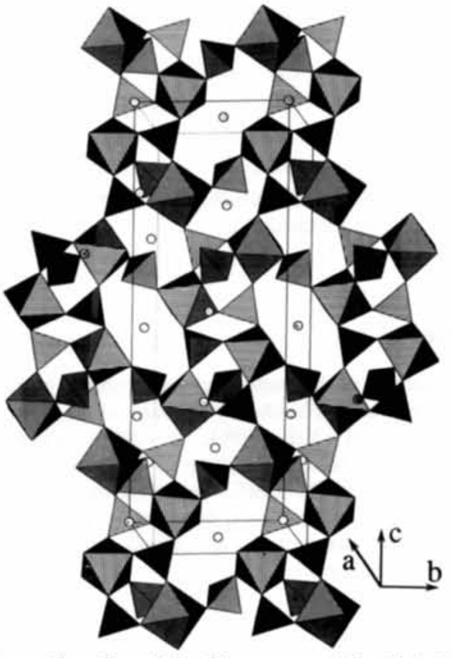

Fig. 1. Perspective view of the title compound. Small circles are Li atoms.

Acta Crystallographica Section C
ISSN 0108-2701 ©1995